

Integrated shadow mask for sampled Bragg gratings in chalcogenide (As_2S_3) planar waveguides

Duk-Yong Choi^{1*}, Steve Madden¹, Andrei Rode¹, Rongping Wang¹, Barry Luther-Davies¹, Neil J. Baker², Benjamin J. Eggleton²

¹Centre for Ultrahigh-bandwidth Devices for Optical Systems (CUDOS)
Laser Physics Centre, Australian National University, Australian Capital Territory 0200, Australia

²Centre for Ultrahigh-bandwidth Devices for Optical Systems (CUDOS)
School of Physics, University of Sydney, New South Wales 2006, Australia

*Corresponding author: dyc111@rsphymail.anu.edu.au

Abstract: We have developed a new approach for producing high performance sampled Bragg gratings in planar waveguides as a platform for WDM on-chip signal processing in a compact integrated device. Using this method we have successfully integrated a shadow mask directly onto a chalcogenide (As_2S_3) waveguide using standard semiconductor processing, eliminating misalignment errors between the mask and waveguide that otherwise occur. Through this integrated mask we demonstrate a very low duty cycle sampled Bragg grating with very narrow rejection peaks and spanning a very broad bandwidth.

© 2007 Optical Society of America

OCIS codes: (090.2880) Holographic interferometry; (160.2750) Glass and other amorphous materials; (220.4000) Microstructure fabrication; (230.1480) Bragg reflectors.

References and Links

1. K. O. Hill, Y. Fujii, D. C. Johnson, and B. S. Kawasaki, "Photosensitivity in optical fiber waveguides: application to reflection fiber fabrication," *Appl. Phys. Lett.* **32**, 647-649 (1978).
2. B. J. Eggleton, P. A. Krug, L. Poladian, and F. Ouellette, "Long periodic superstructure Bragg gratings in optical fibres," *Electron. Lett.* **30**, 1620-1622 (1994).
3. A. Othonos, "Fiber Bragg gratings," *Rev. Sci. Instrum.* **68**, 4309-4341 (1997).
4. J.M. Harbold, F.O. Ilday, F.W. Wise and B.G. Aitken, "Highly nonlinear Ge-As-Se and Ge-As-S-Se Glasses for all-optical switching," *IEEE Photon. Technol. Lett.* **14**, 822-824 (2002).
5. J.T. Gopinath, M. Solajcic and E. Ippen, V. N. Fuflygin, M. Shurgalin "Third order nonlinearities in Ge-As-Se based glasses for telecommunications applications," *J. Appl. Phys.* **96**, 6931-6933 (2004).
6. J.M. Harbold, F.Ö. Ilday, F.W. Wise, J.S. Sanghera, V.Q. Nguyen, L.B. Shaw and I.D. Aggarwal, "Highly nonlinear As-S-Se glasses for all-optical switching," *Opt. Lett.* **27**, 119-121 (2002).
7. K. Tanaka, N. Toyosawa, and H. Hisakuni, "Photoinduced Bragg gratings in As_2S_3 optical fibers," *Opt. Lett.* **20**, 1976-1978 (1995).
8. C. Meneghini and A. Villeneuve, "As₂S₃ photosensitivity by two-photon absorption: holographic gratings and self-written channel waveguides," *J. Opt. Soc. Am. B* **15**, 2946-2950 (1998).
9. T. V. Galstyan, J.-F. Viens, A. Villeneuve, K. Richardson, and M. A. Duguay, "Photoinduced Self-Developing Relief Gratings in Thin Film Chalcogenide As_2S_3 Glasses," *J. Lightwave Technol.* **13**, 1343-1347 (1997).
10. M. Shokooh-Saremi, V. G. Ta'eed, N. J. Baker, I. C. M. Littler, D. J. Moss, B. J. Eggleton, Y. Ruan, and B. Luther-Davies, "High-performance Bragg gratings in chalcogenide rib-waveguides written with a modified Sagnac Interferometer," *J. Opt. Soc. Am. B* **23**, 1323-1331 (2006).
11. A. Zoubir, M. Richardson, C. Rivero, A. Schulte, C. Lopez, K. Richardson, N. Hô, and R. Vallée, "Direct femtosecond laser writing of waveguides in As_2S_3 thin films," *Opt. Lett.* **29**, 748-750 (2004).
12. N. J. Baker, H. W. Lee, I. C. M. Littler, C. M. de Sterke, B. J. Eggleton, D.-Y. Choi, S. Maden, B. Luther-Davies "Sampled Bragg gratings in chalcogenide (As_2S_3) rib waveguides," *Opt. Express* **14**, 9451-9459 (2006).
13. B. Luther-Davies, V. Z. Kolev, M. J. Lederer, N. R. Madsen, A. V. Rode, J. Gieseckus, K.-M. Du, M. Duering, "Table-top 50-W laser system for ultra-fast laser ablation," *Appl. Phys. A* **79**, 1051-1055 (2004).
14. B. Luther-Davies, A. V. Rode, N. Madsen, E. G. Gamaly, "Picosecond high repetition rate pulsed laser ablation of dielectrics: The effect of energy accumulation between pulses," *Opt. Eng.* **44**, 51102-1-8 (2005).

15. Inorganic Polymer Glass is a trade mark of RPO Pty, Ltd. of Canberra, Australia.
16. D. Y. Choi, S. Madden, A. Rode, R. Wang, B. Luther-Davies, "Fabrication and optical characterisation of $\text{Ge}_{33}\text{As}_{12}\text{Se}_{55}$ (AMTIR-1) Thin Film Waveguides," Proc. of IEEE LEOS 2006, 318-319 (2006).

1. Introduction

Bragg gratings have been widely researched and exploited in optical communication system and sensors since the first in-fiber Bragg grating was demonstrated by Hill *et al.* in 1978 [1]. Sampled Bragg Gratings (SBGs) are one of many novel Bragg grating structures where the amplitude or phase of the refractive index change is modulated periodically along the structure. Such a grating can be fabricated by modulating the exposure of the waveguide to the grating writing beams along the waveguide using, for example, a shadow mask. An approach used by Eggleton *et al.* [2] involved translating the UV writing beams along a fiber and phase-mask assembly while the intensity of the beam was modulated. Given a modulation period P , the reflection spectrum of such a grating consists of multiple reflection peaks separated by $\Delta\lambda = \lambda_B^2/2nP$, where λ_B is the central Bragg wavelength, and n is the effective refractive index. These super-structure gratings can be used as comb filters for signal processing and for increasing the tunability of a fiber laser grating reflector [3].

The overall bandwidth of the transmission dips is governed approximately by the Fourier transform of the envelope of the sampled "on" part, making the bandwidth roughly inversely proportional to the duty cycle; while the depth of the individual transmission dips is proportional to the product of the index modulation (Δn) and the effective grating length ($L \times$ duty cycle). Hence, to produce a SBG combining a broad bandwidth with deep transmission dips requires not only a very small duty cycle, but also a large Δn and/or L . However, in order to integrate SBGs into compact on-chip devices, L needs to be kept small. Here we, therefore, utilize the huge photo-induced refractive index change of chalcogenide glass to compensate for a short grating length.

Chalcogenide glasses, which contain the chalcogen elements S, Se, and Te covalently bonded to network forming elements such as Ge, As, Sb, Si, have attractive properties for a wide range of photonic applications. In particular their large linear and nonlinear refractive index makes them suitable for fabricating highly nonlinear photonic wire waveguides [4-6]; the sensitivity to band-edge light makes it easy to photo-define Bragg gratings into the material [7-10]; their vibrational absorption bands lie well into the mid-IR (beyond $8\mu\text{m}$) making them suitable hosts for rare earth dopants; and high third order nonlinearity suggests they can be used as compact Raman amplifiers. Even though there is still some uncertainty on the mechanism of the photo-induced refractive index change in chalcogenides, large index changes have been reported -10^{-3} to 10^{-1} [11] – which is at least an order of magnitude larger than that in Ge-doped silica fiber.

In this work we focus on the production of broadband comb filters based on SBGs written into chalcogenide waveguides using the large photosensitivity of As_2S_3 glass to 532 nm laser light. In order to eliminate errors introduced in the grating writing process by misalignment of an external shadow-mask required to create the grating, we demonstrate here a novel approach and integrate the mask directly onto the waveguide chip. Such comb filters may be used to produce multi-line emission from rare earth doped chalcogenide waveguide lasers.

2. Background

We have recently reported [12] the production of multi-wavelength comb-filters based on strong SBGs in highly photosensitive As_2S_3 waveguides using a separate amplitude mask to produce the required modulation. An As_2S_3 film deposited by ultra-fast pulsed laser deposition [13-14], was patterned with standard semiconductor processing to produce rib waveguides. Figure 1(a) shows the schematic of the scanning Sagnac interferometer used in combination with a "sampled" shadow mask used to write these gratings. The strength and bandwidth of the SBG reflectivity were comparable to the best ever reported for a silica optical fiber, due to the strong photosensitivity of the chalcogenide glass.

When using a shadow mask placed in close contact to the planar waveguide there is a significant probability that the waveguide will be damaged or contaminated by the mask. In these previous experiments, therefore, the waveguide and mask had to be separated and aligned manually. The arrangement proved very sensitive to the parallelism that could be obtained between the waveguide and the shadow mask, with even a small amount of misalignment causing the overlap of the interfering beams to “walk-off”, as shown in Fig. 1(b). Consequently, this approach limited the length of the SBG and made working with very low duty cycle shadow masks impractical. For example, a mask having 25 μm wide slits and that is misaligned to the waveguide with a tilt of 0.125° limits the grating length to ≈ 8 mm [12]. Additionally, the walk-off effect also varied the effective optical path length between each “on” region of the SBG which in turn chirped the grating, broadening the rejection peaks.

In this paper we introduce a fully integrated approach for fabricating a SBG in planar As_2S_3 waveguides. Our approach employs an on-chip shadow mask structure to achieve near perfect alignment between the mask and the waveguide. The basic approach was to pattern the shadow mask directly on top of a thick waveguide cladding by exploiting a standard semiconductor fabrication process.

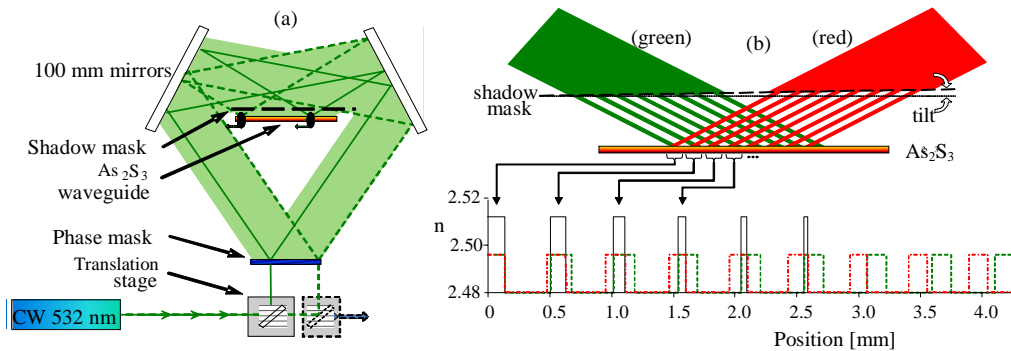


Fig. 1. (a) Scanning Sagnac interferometric grating system showing modulating shadow mask for an SBG fabrication (b) Schematic demonstrating the interference walk-off caused by a tilt of the shadow mask [12].

3. As_2S_3 waveguides, shadow mask and SBG fabrication

Figure 2(a) shows the principle of our new shadow mask. Pairs of adjacent openings were created through which the two beams of the interferometer could enter and interfere in the plane of the As_2S_3 waveguide. The slit width, which is fixed at fabrication, pre-sets the overall bandwidth of the spectrum. Several dozen double-slits were positioned along the waveguide at 500 μm intervals. Spectrally, this corresponds to a ~ 1 nm separation between the rejection peaks around the Bragg wavelength of 1550 nm.

As a consequence of this design, a non-interfering (i.e., DC) index change also occurs on each side of the interference region (two dotted lines in Fig. 2(a)) which causes a minor increase in the effective path length in the waveguide between adjacent interference regions. This results in a slight change in the separation of each rejection peak ($\Delta\lambda$) but has no other impact on the grating performance.

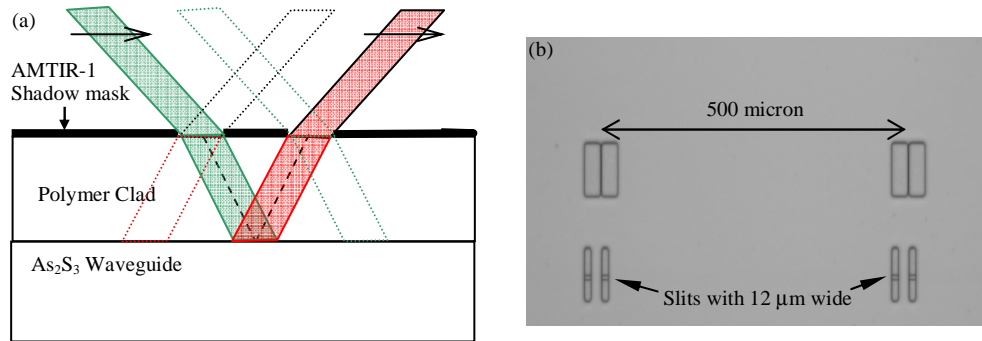


Fig. 2. (a) Schematic showing the principle of this double slits structure (b) The optical microscope image of the fabricated shadow mask on the clad surface. We can see a part of the As_2S_3 waveguide through the slits and polymer cladding.

Figure 2(b) shows an optical microscope image of the fabricated shadow mask on top of the cladding. The As_2S_3 rib waveguide is visible under the 12 micron wide slits. To produce this structure As_2S_3 rib-waveguides were first patterned using standard photolithography and dry etching and then a uniform layer of UV-curable Inorganic Polymer GlassTM [15] was spin coated on top of the rib waveguides to create the cladding. We found that the standard deviation in the cladding thickness across a full 4" wafer was ~ 20 nm when using a 21 μm thick layer. This excellent thickness uniformity ensured there was a negligible tilt between the shadow mask integrated on top of the cladding and the waveguides over the whole wafer.

The mask itself comprised a patterned 1 μm thick layer of $\text{Ge}_{33}\text{As}_{12}\text{Se}_{55}$ (AMTIR-1) amorphous film [16] coated by pulsed laser deposition onto the cladding. AMTIR-1 is strongly absorbing at 532 nm – the wavelength used to write the gratings – having only 0.1% transmission at this thickness. The absorbing nature of AMTIR-1 helped minimize multiple reflections that would otherwise occur between the highly reflective Si substrate and the mask layer, preserving the quality of the grating. We plasma-etched the AMTIR-1 after photo-resist patterning to open the slits. We made a slanted etch profile to reduce screening of the incoming beam by the edge of the shadow mask. This could be achieved by using pure CF_4 plasma gas which provided isotropic etching creating a slanted wall [16].

The SBG writing process was the same as used in the earlier work [12], except now the shadow mask was integrated directly onto the waveguide chip. The rib width, rib height, and slab height of the waveguide were 4, 2.5, and 1.5 micron, respectively. The slit opening on the shadow mask was 12 micron (2.4% duty cycle). The output of the writing laser was spatially filtered and then collimated to a diameter of 0.5 mm with each interfering arm carrying 3 mW of optical power. The writing beams were scanned across the waveguide with a uniform speed of 10 $\mu\text{m}/\text{sec}$ for 60 minutes to pattern a 36 mm SBG.

4. Optical characterization and analysis

The spectral response of the SBG so-written into the As_2S_3 waveguide is shown in Fig. 3. This spectrum has a 3 dB bandwidth of almost 60 nm, with a central peak at 1551 nm. Compared to our earlier result [12], in which the slit width was 25 μm (for a duty cycle of 5%), the bandwidth has been increased by more than 20 nm, although the depth of reflection peaks are less strong, as would be expected for a similar SBG with a lower duty cycle. The most noticeable improvement in the present work was the sharpness of each rejection peak in the spectrum. The inset in Fig. 3 (right side) shows the enlarged view of the peak at 1551 nm. The average 3 dB bandwidth of the peaks was only 150 pm. We attribute this improvement to the elimination of chirp resulting from the near ideal shadow mask structure. The ripples in the transmission spectrum are due to Fabry-Perot effects from the waveguide end facets, which we believe can be eliminated by applying anti-reflection coatings to the facets.

The elimination of tilt between the waveguide and shadow mask is the major advantage of using an integrated mask to produce the SBG. In optimal conditions spin-coating can routinely produce claddings on top of a patterned waveguide uniform to better than 0.1 % over the full area of the wafer. The excellent parallelism between the waveguide and mask would be almost impossible to achieve using a separate, manually-aligned mask. This integrated mask thus allows the fabrication of longer gratings which produces stronger reflection peaks in the spectrum, whilst the overall bandwidth can be simultaneously extended by employing low duty cycle, i.e., small slit widths. In our previous SBG scheme using a separate mask, therefore, mask openings smaller than 25 micron are not practical whereas 12 microns was easily achieved in the integrated mask. The negligible tilt also results in the very sharp rejection peaks as shown in Fig. 3 due to the elimination of chirp in the system.

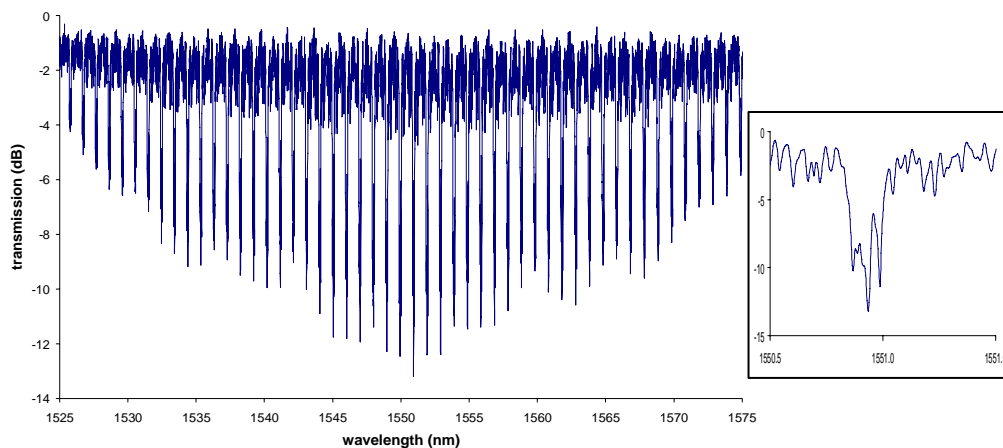


Fig. 3. The spectral response of a SBG written into an As_2S_3 waveguide. The inset in right side shows the enlarged view of the peak centered at 1551 nm.

5. Conclusion

We have demonstrated that by integrating a shadow mask directly onto the waveguide chip we can eliminate error in the SBG caused by misalignment between an external shadow mask and the waveguide thereby eliminating beam walk-off. As a consequence, we were able to obtain very narrow rejection peaks and extend the usable bandwidth. This technique ensures the reliable production of long SBGs with a small duty cycle enabling uniformly strong rejection peaks over a very broad bandwidth. These filters are well suited for applications such as on-chip multi-wavelength Raman lasers. The same scheme should allow for fabrication of high quality multi-phase shifted Bragg gratings and long-period gratings using conventional grating writing systems.

Acknowledgments

This work was produced with the assistance of the Australian Research Council (ARC). The Centre for Ultrahigh-bandwidth Devices for Optical Systems (CUDOS) is an ARC Centre of Excellence.